

## Interpretation of the solution properties of Fe-Mg olivines and aqueous Fe-Mg chlorides from ion-exchange experiments

PAUL R. BARTHOLOMEW

Department of Earth and Space Sciences, State University of New York, Stony Brook, New York 11794, U.S.A.

### ABSTRACT

The ion-exchange equilibrium between synthetic Fe-Mg olivines and 2 molal Fe-Mg chloride aqueous solutions has been bracketed between 450 and 800 °C and between 1 and 4 kbar. Additional experiments at lower chloride molalities reveal that the measured distribution coefficient is dependent upon chloride concentration. A detailed aqueous solution model that accounts for the distribution of neutral and charged aqueous species shows that contrasts in the dissociation equilibria of the Fe and Mg chlorides can account for the observed concentration dependence. A tentative value for the first dissociation constant for FeCl<sub>2</sub> calculated from the experimental data requires an unexpectedly low hydration number (between 3 and 4). An internally consistent thermodynamic solution model for Fe-Mg olivine is presented; this model was calculated by linear programming from the ion-exchange data and constrained by published independent data. Conflicts between fitting the ion-exchange data and calorimetric constraints on the olivine solution model lead to uncertainties in the accuracy of the employed aqueous solution model. The demonstrated effects of partial dissociation along with unresolved uncertainties in the aqueous solution model indicate that previous solid solution models derived from ion-exchange equilibria with aqueous chlorides may be in error.

### INTRODUCTION

Experimental and theoretical investigation of the Fe-Mg olivine solid solution has received considerable attention in the literature. Most of the experimental contributions are Fe-Mg ion-exchange experiments. Included are studies of the exchange equilibrium with orthopyroxene (Nafziger and Muan, 1967; Kitayama and Katsura, 1968; Medaris, 1969; Williams, 1971; Matsui and Nishizawa, 1974), garnet (Kawasaki and Matsui, 1977; O'Neill and Wood, 1979; Kawasaki and Matsui, 1983), spinel (Engi, 1978, 1983), ilmenite (Andersen and Lindsley, 1979, 1981), calcic olivine (Davidson and Mukhopadhyay, 1984), and Fe-Mg chloride aqueous solutions (Schulien et al., 1970). Contributions using calorimetry include Sahama and Torgeson (1949), Wood and Kleppa (1981), and Thierry et al. (1981). Additional efforts to analyze (or reanalyze) portions of the experimental data include work by Williams (1972), Saxena (1972), Obata et al. (1974), Engi (1980a), and Sack (1980). The investigation presented here was aimed at making two contributions: (1) To extend an olivine solution model with confidence down to temperatures where olivine is important as a metamorphic mineral. (2) To critically evaluate the utility of aqueous chlorides, particularly Fe-Mg chlorides, for characterizing solid solutions through ion-exchange experiments.

Of the above exchange equilibrium experimental studies, only Schulien et al. (1970) and Andersen and Lindsley (1979) provided data below 800 °C that span the Fe-

Mg composition range. The Fe-Mg exchange equilibrium experiments reported here were performed over a range of conditions from 450 to 800 °C and 1 to 4 kbar using 2*m* aqueous Fe-Mg chloride solutions as the second phase. Although Schulien et al. (1970) performed similar experiments under similar conditions, the size of their compositional error brackets restricts their study to qualitative characterization of the olivine solid solution. To help evaluate the role of the chloride solution in the study presented here, additional experiments were conducted at constant olivine starting composition while varying the total concentration of chlorides.

Aqueous chlorides have been in use as ion-exchange media for over 20 years. Ion-exchange studies that consider aqueous chlorides as an equilibrium phase include Orville (1963; alkali feldspar), Schulien et al. (1970; olivine), Wellman (1970; sodalite), Orville (1972; plagioclase), Lagache and Weisbrod (1977; alkali feldspar), Ellis (1978; scapolite), Perchuk and Aranovich (1979; Ca garnet, epidote), Schulien (1980; biotite), and Pascal and Roux (1985; muscovite-paragonite).

The attractions of aqueous chlorides as an exchange medium include faster reaction rates compared to solid-solid reactions, an assumed lack of compositional inhomogeneity in the aqueous solution, ease of phase separation for independent chemical analysis, and the common assumption that the mixture of chlorides in supercritical aqueous solution could be treated as an "ideal" solution. Engi (1980b) pointed out the fallacy of this

last assumption for Fe-Mg chloride solutions, and Pascal and Roux (1985) have calculated effective bulk excess mixing properties of supercritical NaCl-KCl solutions.

## EXPERIMENTAL TECHNIQUES

### Starting materials

Synthetic olivines were made from reagent-grade oxides at composition intervals of 0.1  $X_{\text{Fe}}$  (mole fraction of the forsterite end-member). The Fe-bearing olivines were synthesized from oxygen-balanced mixes in evacuated silica-glass tubes at 1050 °C (method 2 of Turnock et al., 1973). The Mg end-member mix was heated in air at 1400 °C for 24 h, ground, and heated for another 24 h. All synthesis products were examined both optically and by XRD and found to contain 99% or more olivine. Grain sizes ranged from <2  $\mu\text{m}$  for the magnesian compositions to 1–5  $\mu\text{m}$  for the Fe-rich compositions.

End-member chloride solutions at 2*m* concentration were prepared from reagent-grade  $\text{MgCl}_2 \cdot 6\text{H}_2\text{O}$  and  $\text{FeCl}_2 \cdot 4\text{H}_2\text{O}$  and distilled water. Intermediate-composition solutions were prepared by mixing the end-members. The Fe and Mg concentrations in each of these solutions were checked by standard flame atomic absorption. In some cases, solutions of intermediate composition were created in the run capsule by pipetting small aliquots of the end-member solutions into the capsule and carefully weighing each aliquot. Run solutions at concentrations less than 2*m* were created the same way, using distilled water as one aliquot. Densities determined by weighing known volumes of the end-member solutions allowed conversion of weights to volumes and conversion of molality to molarity when needed.

### Ion-exchange experiments

Weighed amounts of olivine and chloride solution (30–100 mg of each) were sealed into noble-metal capsules. Au capsules were used above 600 °C, both Au and  $\text{Ag}_{60}\text{Pd}_{40}$  capsules were used at 600 °C, and both  $\text{Ag}_{60}\text{Pd}_{40}$  capsules and thin-walled (0.1 mm) Au capsules were used below 600 °C. All runs were made in 3.2 × 30.5 cm cold-seal pressure vessels heated within horizontal furnaces. A quick-quench configuration employing a short (5 cm) filler rod as the sole modification was used above 600 °C so that the capsule could be dropped close to the cool end of the bomb (see also Wellman, 1970). Quench time for all runs was reduced, compared to a standard compressed-air quench, by aspirating water into the air stream. Run temperature was measured with a calibrated chromel-alumel thermocouple inserted into an external well in each bomb. The combination of all calibration, spatial variation, and time-variation temperature errors is estimated to be no more than ±5 °C. The pressure medium was methane for the 1- and 2-kbar runs. The  $\text{H}_2$  pressure established by the graphite-methane equilibrium prevented oxidation of the capsule contents for runs at and above 600 °C. Below 600 °C, a higher  $\text{H}_2$  pressure was needed to keep  $f_{\text{O}_2}$  in the capsule below that of the fayalite-magnetite-quartz buffer. To accomplish this,  $\text{H}_2$  was introduced into the bomb before pressurizing with methane, and graphite was not introduced. The amount of  $\text{H}_2$  added was designed to result in a  $\text{H}_2$  partial pressure between values calculated for the fayalite-magnetite-quartz- $\text{H}_2\text{O}$  equilibrium and the magnetite-wüstite- $\text{H}_2\text{O}$  equilibrium. Some  $\text{H}_2$  was also introduced in runs above 600 °C to minimize the amount of graphite precipitation since this precipitated graphite was found to impede “drop” quenching. The runs at 4 kbar were pressurized with water. For these runs a button of graphite introduced along with the run capsule was found to prevent oxidation at 600 °C. Pressure on the methane line was measured with an

Ashcroft gauge calibrated against a factory-calibrated 2000-bar Heise gauge. At 4 kbar, pressure was measured with a 7000-bar Heise gauge. Stated pressures are considered accurate to within 60 bars.

Following each experiment, the capsule was cleaned, weighed, punctured with a needle at both ends and placed in an Ar-flushed 1-mL centrifuge vial. The vial was sealed and centrifuged. Typically, 50 to 70% of the run fluid was extracted, and any solids extracted with the fluid were simultaneously separated. The portion of the extracted fluid that could be drawn off uncontaminated by solids was diluted with slightly acidified (0.03*M*  $\text{HNO}_3$ ) distilled water in preparation for chemical analysis. Whenever sufficient fluid could not be extracted by centrifuging, the capsule was cut open and the contents washed into the centrifuge vial with distilled water. The vial was sealed, agitated, and centrifuged, and the supernatant liquid was drawn off and diluted with acidified water. The solid products of each experiment were washed with distilled  $\text{H}_2\text{O}$ , centrifuged, washed with alcohol, centrifuged, and dried.

### Final compositions

The concentrations of Fe and Mg in the diluted product solutions were measured with standard acetylene-flame atomic-absorption techniques. For a representative portion of the experiments, total Cl was measured with a Buchler-Cotlove chloridometer. For a small number of experiments at each set of conditions, quench pH was measured directly on the separated fluid immediately after centrifuging. A microcombination pH electrode was inserted into the vial through a collar that was continuously flushed with Ar. The quench pH was found to be nearly constant ( $5.3 \pm 0.5$ ) at all sets of conditions except for the single measurement made at 800 °C (3.86).

All solid products were examined optically, and many were checked with XRD. In addition to olivine, the solid products of a majority of the ion-exchange experiments included a silicate more siliceous than olivine. This additional phase was either quartz, talc, orthopyroxene, or orthoamphibole, and its modal amount was generally less than 2%, but occasionally up to 5%. The presence of these siliceous accessory phases was attributed to incongruent dissolution of the olivine into the aqueous solution at *P* and *T*. Because the concentration of aqueous Cl is constant, nonchloride species of Mg and/or Fe must have been present at *P* and *T*. Traces of a green, amorphous substance found in many of the experimental run products may be a precipitate formed from these nonchloride species upon quenching. Total Cl measurements generally indicated that only chloride species remained in solution after quenching. Expressed in terms of percent departure from  $\text{MgCl}_2$  stoichiometry ( $= 100 \times \{[2(\text{Fe} + \text{Mg})/\text{Cl}] - 1\}$ ), the average values are 6% ± 5% (450 °C, 1 kbar), 1% ± 5% (600 °C, 1 kbar), 1% ± 5% (600 °C, 2 kbar), 6% ± 5% (600 °C, 4 kbar), 2% ± 2% (725 °C, 2 kbar).

Final olivine compositions were established initially by mass balance and then finally by one or more of three electron-microprobe techniques. The three microprobe techniques that were employed are standard analysis, particle analysis, and crystal-face analysis. For standard analysis, product olivine grains were hot-pressed into Buehler Transoptic plastic and polished with diamond abrasives. Synthetic end-member olivine grains (50 to 150  $\mu\text{m}$ ), identically mounted, were used as standards, and the correction procedures of Bence and Albee (1968) and Albee and Ray (1970) were used. The operating conditions were 15 kV with 15-nA specimen current. Mg, Fe, and Si were analyzed simultaneously employing 20-s counting times. For each sample, 6 to

10 analyses were averaged. Some of the analyses were done on an automated ARL-EMX at the University of Washington, Seattle, and the remainder were done at the University of British Columbia on an ARL-SEM-Q. Standard analysis was judged inadequate for a majority of the samples for two reasons: (1) The olivine grain size in some samples was too small to contain the beam and its excitation volume. (2) Compositional zoning was inferred to be present in many samples.

Compositional zoning was inferred to be present by comparing mass-balance and standard microprobe analyses. For 15 to 25  $\mu\text{m}$  grains (a very common size range), only core analyses would produce acceptable totals and stoichiometry. The microprobe composition ( $X_{\text{fo}}$ ) of such grains was generally between the mass-balance  $X_{\text{fo}}$  and the initial  $X_{\text{fo}}$ . Since this relationship persisted independently of the direction of approach toward the final composition, the potential effect of precipitates and non-olivine silicates on the mass-balance composition could be eliminated as the cause. For grains larger than 25  $\mu\text{m}$ , analyses were taken as close as possible to grain edges, but, once again, edge zoning on a 5- $\mu\text{m}$  scale could not be measured directly. To eliminate minimum grain size and fine-scale zoning problems, many samples were analyzed with particle-analysis techniques. The olivine grains were dispersed on polished graphite stubs and carbon coated. While operating at 15 kV and 35 nA on the ARL-SEM-Q, the beam was rastered over a 10- $\mu\text{m}$  square. Secondary electron imaging made it possible to select grains entirely containable within the 10- $\mu\text{m}$  square for analysis. Mg, Fe, and Si were analyzed simultaneously employing 40-s counting times. A first approximation of particle composition was established using the same standardization and correction procedures described above for standard analysis. An empirical correction curve was established by using the same procedures to analyze all of the synthetic olivines used as starting materials. Each particle analysis reported is an average of 10 to 15 individual analyses.

Some of the higher-temperature run products did not contain olivine grains smaller than 10  $\mu\text{m}$  and could not be analyzed using the same particle-analysis procedures. Edge compositions were measured for several of these large-grain samples using crystal-face analyses: standard analysis techniques on particle analysis mounts. Most of the product olivines were quite euhedral. As a result, many of the grains dispersed for particle analysis lie flat on their largest crystal face: (010). The upper (010) face is then both flat and horizontal. Standard analysis of (010) faces larger than 15  $\mu\text{m}$  across produced acceptable totals and formulae.

### DATA ANALYSIS

Run conditions and compositions for the critical runs are listed in Table 1. Also presented in Table 1 are calculated values of  $\ln K_{\text{D}}$ , where  $K_{\text{D}}$  is the bulk distribution coefficient expressed as

$$K_{\text{D}} = (X_{\text{Mg,aq}}X_{\text{fa}})/X_{\text{Fe,aq}}X_{\text{fo}} \quad (1)$$

where  $X_{\text{Mg,aq}}$  and  $X_{\text{Fe,aq}}$  are the mole fractions of Mg and Fe in the aqueous solution, respectively, and  $X_{\text{fo}}$  and  $X_{\text{fa}}$  are the mole fractions of forsterite and fayalite in the olivine. Any variation in  $K_{\text{D}}$  with variations in phase compositions at constant  $T$  and  $P$  indicates "nonideal mixing" (in terms of bulk properties) in one or both of the solution phases. Any variation in  $K_{\text{D}}$  at constant  $T$ ,  $P$ , and  $X_{\text{fo}}$  with variation in total chloride concentration can only be attributed to the aqueous solution. Plots of  $\ln K_{\text{D}}$

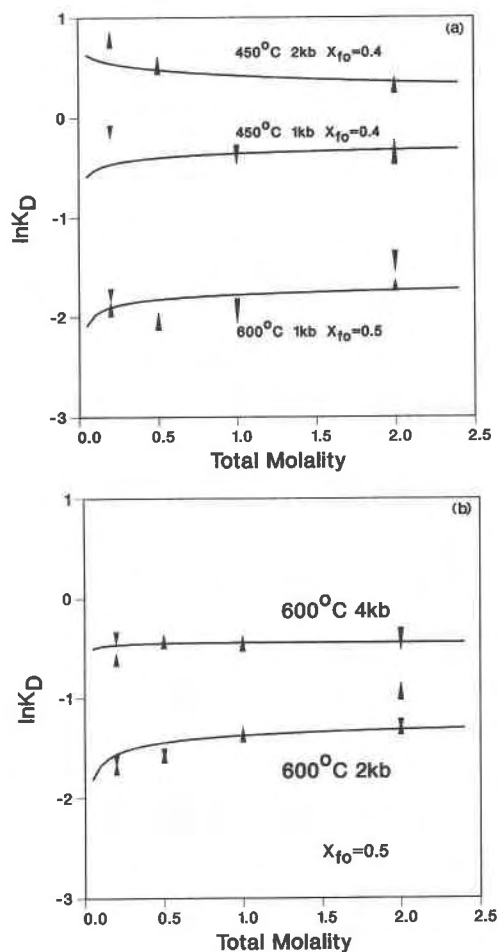


Fig. 1.  $\ln K_{\text{D}}$  vs.  $m_{\text{T}}$  for isothermal-isobaric-iso- $X_{\text{fo}}$  subsets of the ion-exchange experiments. The symbols marking each experimental measurement point in the direction of approach toward equilibrium. The measurement itself is at the center of the symbol and the length and width of the symbol represent  $\pm 1\sigma$ . Minor deviations in measured  $X_{\text{fo}}$  from the stated constant value have been corrected for the purpose of illustration by adjusting  $\ln K_{\text{D}}$  parallel to the regressed model for  $\ln K_{\text{D}}$  as a function of  $X_{\text{fo}}$ . The solid lines illustrate the regressed model of  $\ln K_{\text{D}}$  as a function of  $m_{\text{T}}$ . (a) Data at 450 °C (1 and 2 kbar) and 600 °C (1 kbar). (b) Data at 600 °C (2 and 4 kbar).

subgroups of the data at constant  $X_{\text{fo}}$  (Fig. 1) show that such variations in  $K_{\text{D}}$  with total chloride molality exist. The role of the aqueous solution in the ion-exchange experiments must therefore be examined before the properties of the olivine solution can be examined.

### The aqueous solution

At supercritical temperatures and moderate pressures, aqueous electrolytes are present in solution dominantly as neutral species, but partially as charged species derived through dissociation reactions. Figure 2 illustrates the available data for the conventional molal dissociation constant for chloride compounds at  $P$ - $T$  conditions per-

TABLE 1. Ion-exchange run data

Run	T (°C)	P (kbar)	t (h)	Initial			Final			ln $K_D(1\sigma)$	ln $K_D^0$
				$X_{Co}$	$X_{Mg}$	$m_T$	$X_{Mg}$	$X_{Co}$			
142	450	1	996	0.4	0.0	2.0	0.296	0.338	-0.19(10)	0.01	
143	450	1	996	0.4	0.7	1.0	0.334	0.455	-0.51(07)	-0.28	
145	450	1	1000	0.1	0.5	2.0	0.251	0.163	0.54(07)	0.74	
146	450	1	1000	0.7	0.7	2.0	0.504	0.728	-0.97(07)	-0.76	
147	450	1	1000	1.0	0.7	2.0	0.759	0.984	-2.97(64)	-2.75	
163	450	1	840	0.1	0.0	2.0	0.094	0.074	0.26(17)	0.45	
164	450	1	840	0.4	0.5	0.2	0.374	0.419	-0.19(06)	0.16	
165	450	2	842	0.4	0.1	2.0	0.450	0.334	0.49(06)	0.48	
166	450	2	842	0.4	0.1	0.5	0.506	0.347	0.66(07)	0.52	
167	450	2	842	0.4	0.5	0.2	0.588	0.388	0.81(08)	0.61	
116	600	1	510	0.5	0.1	2.0	0.152	0.492	-1.69(06)	-1.48	
117	600	1	528	0.5	0.5	0.2	0.146	0.504	-1.78(06)	-1.40	
121	600	1	435	0.5	0.0	0.2	0.120	0.478	-1.90(06)	-1.52	
122	600	1	436	0.5	0.5	2.0	0.205	0.529	-1.47(09)	-1.25	
124	600	1	436	0.8	0.5	2.0	0.411	0.807	-1.79(07)	-1.56	
135	600	1	650	0.5	0.5	1.0	0.156	0.582	-2.02(10)	-1.76	
136	600	1	650	0.5	0.0	0.5	0.106	0.472	-2.02(08)	-1.72	
199	600	1	627	0.1	0.3	2.0	0.040	0.123	-1.21(08)	-1.00	
200	600	1	627	0.3	0.3	2.0	0.095	0.327	-1.53(11)	-1.32	
25	600	2	240	0.1	0.1	2.0	0.070	0.101	-0.40(07)	-0.23	
26	600	2	240	0.3	0.2	2.0	0.157	0.299	-0.83(11)	-0.65	
27	600	2	240	0.3	0.0	2.0	0.138	0.270	-0.84(10)	-0.66	
37	600	2	338	0.6	0.3	2.0	0.265	0.607	-1.46(07)	-1.27	
38	600	2	338	0.7	0.1	2.0	0.275	0.679	-1.72(08)	-1.53	
39	600	2	697	0.8	0.2	2.0	0.359	0.770	-1.79(07)	-1.59	
40	600	2	697	0.8	0.5	2.0	0.443	0.792	-1.57(08)	-1.36	
41	600	2	697	0.9	0.4	2.0	0.524	0.882	-1.92(08)	-1.70	
42	600	2	697	0.9	0.7	2.0	0.617	0.909	-1.83(13)	-1.60	
43	600	2	360	0.5	0.0	2.0	0.200	0.465	-1.25(06)	-1.06	
64	600	2	1212	0.8	0.9	2.0	0.685	0.942	-2.02(19)	-1.78	
66	600	2	1436	0.5	0.3	2.0	0.219	0.500	-1.29(07)	-1.11	
67	600	2	1436	0.5	0.0	0.2	0.154	0.501	-1.71(07)	-1.28	
68	600	2	1436	0.5	0.5	0.2	0.166	0.503	-1.63(07)	-1.20	
119	600	2	435	0.5	0.5	0.5	0.184	0.533	-1.62(06)	-1.31	
133	600	2	758	0.5	0.0	1.0	0.189	0.463	-1.31(06)	-1.07	
134	600	2	758	0.5	0.0	0.5	0.165	0.482	-1.55(06)	-1.24	
101	600	4	382	0.5	0.0	2.0	0.269	0.474	-0.90(08)	-0.81	
102	600	4	382	0.5	0.0	0.2	0.352	0.503	-0.62(06)	-0.51	
103	600	4	382	0.5	0.5	0.2	0.387	0.472	-0.35(06)	-0.24	
128	600	4	385	0.5	0.5	2.0	0.410	0.519	-0.44(10)	-0.35	
129	600	4	385	0.5	0.1	1.0	0.369	0.465	-0.40(07)	-0.31	
130	600	4	385	0.5	0.1	0.5	0.376	0.469	-0.38(06)	-0.29	
174	600	4	601	0.9	0.3	2.0	0.577	0.855	-1.46(09)	-1.38	
197	600	4	530	0.1	0.0	2.0	0.060	0.078	-0.28(11)	-0.20	
225	600	4	579	0.1	0.3	2.0	0.126	0.130	-0.04(13)	0.05	
226	600	4	579	0.3	0.0	2.0	0.189	0.270	-0.46(08)	-0.38	
227	600	4	579	0.8	0.9	2.0	0.598	0.820	-1.12(09)	-1.03	
69	725	2	1106	0.1	0.0	2.0	0.023	0.102	-1.58(12)	-1.39	
70	725	2	1106	0.1	0.1	2.0	0.024	0.107	-1.58(07)	-1.39	
71	725	2	1106	0.4	0.3	2.0	0.089	0.423	-2.02(06)	-1.82	
72	725	2	1105	0.8	0.5	2.0	0.308	0.811	-2.27(06)	-2.06	
211	725	2	351	0.8	0.1	2.0	0.287	0.780	-2.18(08)	-1.97	
212	725	2	351	0.6	0.3	2.0	0.175	0.623	-2.05(06)	-1.85	
213	725	2	351	0.4	0.0	2.0	0.088	0.392	-1.90(07)	-1.70	
75	800	2	1101	0.1	0.1	2.0	0.031	0.105	-1.30(07)	-1.12	
169	800	2	494	0.8	0.7	2.0	0.404	0.877	-2.35(07)	-2.16	
170	800	2	494	0.8	0.1	2.0	0.329	0.825	-2.26(07)	-2.07	
202	800	2	256	0.1	0.0	2.0	0.015	0.113	-2.12(06)	-1.95	
203	800	2	256	0.4	0.3	2.0	0.083	0.420	-2.08(06)	-1.89	
204	800	2	256	0.7	0.5	2.0	0.244	0.745	-2.20(08)	-2.02	

tinant to this study. The conventional molal dissociation constant has the form

$$K_{M,diss} = (m_{M^+}) (m_{Cl^-}) \gamma_{\pm}^2 / m_{MCl} \quad (2)$$

for the generalized 1:1 chloride compound MCl. The curves in Figure 2 were generated with the empirical function used by Frantz and Marshall (1982):

$$\log K_{M,diss} = a + b/T + c \log \rho_w, \quad (3)$$

where  $K_{M,diss}$  is a dissociation equilibrium constant on the molarity concentration scale,<sup>1</sup>  $T$  is in kelvins,  $\rho_w$  is the density of pure H<sub>2</sub>O at  $P$  and  $T$  of interest, and  $a$ ,  $b$ , and  $c$  are empirical fit parameters. The dissociation constants represented by the solid curves have been derived from

<sup>1</sup> In the absence of solution-density measurements at  $P$  and  $T$ , concentration-scale conversions have been made with the dilute solution approximations:  $M_i = m_i \rho_w$  and  $X_i = m_i / 55.51$ .

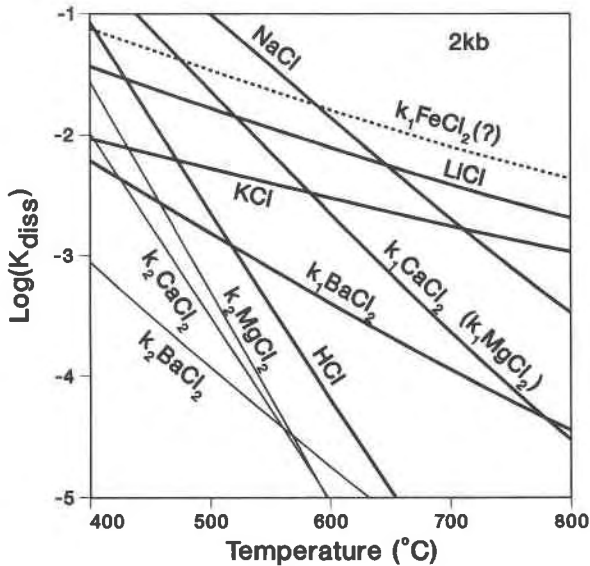


Fig. 2. Common logarithm of aqueous-chloride dissociation constants at 2 kbar. See text for explanations and Table 2 for references.

electrical conductivity measurements by the authors listed in Table 2. Portions of some of the curves in Figure 2 extend beyond the data from which they were derived.

Unfortunately, the data available on the behavior of  $MgCl_2$  in supercritical  $H_2O$  are incomplete, and supercritical data for  $FeCl_2$  solutions are scant. For the dichlorides, therefore, two dissociation constants have been calculated, one for each of two step-wise dissociation reactions:  $MCl_2 = MCl^+ + Cl^-$  and  $MCl^+ = M^{2+} + Cl^-$ . Experimental difficulties attributed to hydrolytic precipitation of  $MgO$  or  $Mg(OH)_2$  prevented Frantz and Marshall (1982) from directly measuring the first dissociation constant of  $MgCl_2$ . They inferred from what data they did gather that  $K_{1,MgCl_2}$  could be treated as identical to  $K_{1,CaCl_2}$ . Only qualitative information is available for the dissociation equilibria of aqueous  $FeCl_2$ . Solubility studies of magnetite (Chou and Eugster, 1977) and hematite (Boctor et al., 1980) in supercritical iron chloride solutions were interpreted by their authors to indicate that associated  $FeCl_2$  is the dominant aqueous species from 400 to 650 °C at 2 kbar and from 400 to 600 °C at 1 kbar. The curve for  $K_{1,FeCl_2}$  is a tentative estimate derived in the present study in a manner described below.

In examining the properties of the aqueous solution, the role of contrasting electrolyte dissociation must be considered. Thompson and Waldbaum (1968), in analyzing the data of Orville (1963), considered the possibility that KCl and NaCl are partially dissociated to  $Na^+$ ,  $K^+$  and  $Cl^-$ . However they only considered the case in which KCl and NaCl are dissociated to the same extent and proceeded to show that this case was indistinguishable from the "ideal solution" assumption when analyzing the ion-exchange equilibrium. Note that, for several pairs of the chlorides represented in Figure 2, the dissociation

TABLE 2. Fit parameters for Equation 3

	a	b	c	Data source*	Regression to Eq. 3*
HCl	-5.41	3875	14.93	1	1
NaCl	-1.43	1470	10.20	2	6
KCl	-2.68	590	3.26	3	6
LiCl	-2.61	970	3.65	4	6
BaCl <sub>2</sub> : K <sub>1</sub>	-3.97	1530	6.13	3	6
BaCl <sub>2</sub> : K <sub>2</sub>	-6.24	2580	7.39	3	6
CaCl <sub>2</sub> : K <sub>1</sub>	-3.21	2407	10.60	5	5
CaCl <sub>2</sub> : K <sub>2</sub>	-5.05	3112	16.50	5	5
MgCl <sub>2</sub> : K <sub>1</sub>	(-3.21)	(2407)	(10.60)	5	5
MgCl <sub>2</sub> : K <sub>2</sub>	-4.80	3415	19.20	5	5

\* References: 1, Frantz and Marshall (1984); 2, Quist and Marshall (1968); 3, Ritzert and Franck (1968); 4, Mangold and Franck (1969); 5, Frantz and Marshall (1982); 6, This study.

constants may be identical at one temperature and an order of magnitude apart at a temperature 200 °C (or less) away. Engi (1980b) demonstrated the possible implications of contrasting dissociation-equilibrium constants on ion-exchange equilibria by applying qualitative equilibrium-constant data for  $MgCl_2 = Mg^{2+} + 2Cl^-$  (Frantz and Popp, 1979) and  $FeCl_2 = Fe^{2+} + 2Cl^-$  (Boctor et al., 1980) to the olivine exchange-equilibrium data of Schullien et al. (1970). Pascal and Roux (1985) derived bulk thermodynamic excess properties of supercritical solutions of KCl and NaCl by calculating the distribution of neutral and charged species.

In contrast to the approach of Pascal and Roux (1985), the approach used here was to recalculate the experimental data in terms of only the dominant aqueous species (assumed to be the neutral species). For the purposes of performing the distribution-of-species calculations, a model closed system containing 1000 g of  $H_2O$  was assumed, allowing measured molalities to be converted to moles and mole fractions.

The modeled exchange reaction is



$$K_D = [(1 - X_{fo})X_{MgCl_2}]/(X_{fo}X_{FeCl_2}) \quad (5)$$

$$K_E = K_D^*(\gamma_{fa}\gamma_{MgCl_2})/(\gamma_{fo}\gamma_{FeCl_2}). \quad (6)$$

Only the first dissociation reactions for the chlorides were considered. Figure 2 illustrates that this simplification may be justified because, over the temperature range of interest here,  $K_{2,MgCl_2}$  is more than 1 log unit below  $K_{1,MgCl_2}$ . The measured bulk  $K_D$  must then be

$$K_D = [(1 - X_{fo})(X_{MgCl_2} + X_{MgCl^+})]/[X_{fo}(X_{FeCl_2} + X_{FeCl^+})]. \quad (7)$$

In order to use values of the conventional dissociation constant at significant electrolyte concentrations, the "complete" dissociation model (Franck, 1956; Quist and Marshall, 1967, 1968) must be applied. The dissociation reaction is expressed in terms of hydrated electrolyte species, and  $H_2O$  takes part in the reaction. The equilib-

rium constant includes the activity of "free" water, water not bound to the electrolyte species.



$$K_{\text{Mg}} = \frac{X_{\text{MgCl}^+} X_{\text{Cl}^-} (\gamma_{\text{MgCl}^+} \gamma_{\text{Cl}^-})}{X_{\text{MgCl}_2} (\gamma_{\text{MgCl}_2}) (X_w \gamma_w)^g} \quad (9)$$



$$K_{\text{Fe}} = \frac{X_{\text{FeCl}^+} X_{\text{Cl}^-} (\gamma_{\text{FeCl}^+} \gamma_{\text{Cl}^-})}{X_{\text{FeCl}_2} (\gamma_{\text{FeCl}_2}) (X_w \gamma_w)^l} \quad (11)$$

where  $g = e + f - d$  and  $l = k + f - j$ .

Activity coefficients of all neutral species were assumed to be 1.0. Rational activity coefficients for charged species were calculated with an unextended Debye-Hückel expression:

$$\log \gamma = (-Z^2 A \sqrt{I}) / (1 + \hat{a} B \sqrt{I}) \quad (12)$$

where  $Z$  is the ionic charge,  $I$  is the true ionic strength (molarity scale).  $A$  and  $B$  are the Debye-Hückel coefficients, and  $\hat{a}$  is the ion-size parameter. Although Helgeson et al. (1981) have provided an extended Debye-Hückel activity-coefficient equation applicable to any aqueous species over a wide range of  $P$ ,  $T$ , and concentration, a lack of appropriate experimental data to quantify the fit parameters precludes its direct application to the species considered here. As the chlorides are only partially dissociated over the  $P$  and  $T$  of interest here, even a total chloride molality of  $2m$  may imply an ionic strength low enough to justify use of Equation 12. In addition, Wilson (1986) found that ionic activity coefficients in supercritical  $\text{MgCl}_2$  solutions calculated by comparing conductivity and solubility studies agreed well with those calculated with an unextended Debye-Hückel expression. A value of  $\hat{a}$  for the ion-pair  $\text{MgCl}^+ \cdot \text{Cl}^-$  was estimated by combining the crystal radii of  $\text{Mg}^{2+}$  and  $\text{Cl}^-$  (Helgeson and Kirkham, 1976; Table 7), calculating an effective electrostatic radius for  $\text{MgCl}^+$  from this sum (Helgeson and Kirkham, 1976; Eq. 61), and calculating  $\hat{a}$  (Helgeson et al., 1981; Eqs. 124 and 125). Since this value was within 2% of the  $\hat{a}$  derived for  $\text{FeCl}^+ \cdot \text{Cl}^-$  in the same manner, it was deemed unnecessary to use distinct values for the two ion pairs, and their average (5.25 Å) was employed.  $A$  and  $B$  were taken from Helgeson and Kirkham (1974) up to 600 °C and were extended to 800 °C with Equations 2 and 3 of Helgeson and Kirkham (1974) along with  $\text{H}_2\text{O}$  dielectric constants provided by Quist and Marshall (1965).

The activity coefficient for  $\text{H}_2\text{O}$  was calculated with an expression derived via the Gibbs-Duhem relation:

$$\log \gamma_w = \frac{2A}{M_w (\hat{a} B)^2} \left( V - 2 \ln V - \frac{1}{V} \right), \quad (13)$$

where  $V = 1 + \hat{a} B \sqrt{I}$ , and  $M_w$  = molarity of  $\text{H}_2\text{O}$  in the solution.

The measured quantities are  $n_T$  (the total moles of  $\text{Mg} + \text{Fe}$  in aqueous solution) and  $X_{\text{Mg}}$  (the mole fraction of  $\text{Mg}$  with reference to  $\text{Mg} + \text{Fe}$  in the aqueous solution). The mass-balance and charge-balance constraints are

$$n_T = n_{\text{MgCl}_2} + n_{\text{MgCl}^+} + n_{\text{FeCl}_2} + n_{\text{FeCl}^+} \quad (14)$$

$$n_{\text{Cl}^-} = n_{\text{MgCl}^+} + n_{\text{FeCl}^+} \quad (15)$$

$$n_w = 55.51 - \sum_i h_i n_i, \quad (16)$$

where  $h_i$  is the hydration number for electrolyte species  $i$ ,

$$n = n_w + \sum_i n_i, \quad (17)$$

and  $n$ , the total number of moles in the system, enables conversion to mole fraction:  $X_i = n_i / n$ .

Solving the distribution of aqueous species in this system requires values for  $n_T$ ,  $X_{\text{Mg}}$ , each of the dissociation equilibrium constants, and the hydration numbers.  $K_{\text{Mg}}$  can be taken from Frantz and Marshall (1982). Because of the results of combining mass-balance constraints, the only hydration numbers required are those for the neutral molecules ( $d$  and  $j$ ) and the net water molecules consumed ( $g$  and  $l$ ). Quist and Marshall (1968) calculated a hydration number for neutral  $\text{NaCl}$  of 1.8 from solubility data at 700 °C and 1240 bars (Sourirajan and Kennedy, 1962). Quist and Marshall (1968) also showed that the net water consumed in the dissociation reaction (=net water value) is given by the rate of change of the molar dissociation constant with solvent density at constant temperature. This rate is identical to the  $c$  parameter in Equation 3. A review of Table 2 then reveals a net water value of 10.6 for  $\text{MgCl}^+$  and values for other 1:1 chlorides ranging from 3 to 15. In light of this information, hydration numbers  $d$  and  $j$  were set to 2 (by analogy with  $\text{NaCl}$ ), and  $g$  was set equal to 10.6. The remaining unknowns are then  $K_{\text{Fe}}$  and net water value  $l$ . Their values must be estimated or derived from the ion-exchange data. In order to employ the ion-exchange data, we must include  $K_E$ ,  $\gamma_{\text{ro}}$ , and  $\gamma_{\text{ra}}$  in the calculations and solve for them simultaneously.

Figure 3 shows how some of the variables in the system defined above influence values predicted for the bulk olivine exchange  $K_D$ . The illustration is for the hypothetical case in which the olivine solid solution is ideal,  $\ln K_E = -1.0$ ,  $\log K_{\text{Mg}} = -2.0$ ,  $T = 600$  °C, and  $P = 2$  kbar. When the dissociation constants for the two chlorides are equal, the system behaves ideally with  $K_D$  equal to  $K_E$ . For the case of unequal dissociation, the direction of the deviation depends on which chloride is more dissociated, and the magnitude of the deviation depends upon the magnitude of the difference in dissociation constants and the total chloride concentration. The solid curves were calculated using 10 for the net water value  $l$ . The dashed and dotted curves show the effect (holding other variables constant) of changing  $l$  to 5 and 15, respectively. It is particularly important to note in Figure 3a that all of the

curves are close to horizontal except near the Fe-Mg compositional end-members. In other words, variables in the aqueous solution model, as defined above, contribute very little to the apparent variation of  $K_D$  with olivine composition.

The remaining unknowns in the aqueous solution model were estimated via regression to the ion-exchange data using experimental  $P$ ,  $T$ , and final  $X_{fo}$  as independent variables and  $\ln K_D$  as the dependent variable. Linear programming would be more appropriate for fitting thermodynamic models to bracket data (Gordon, 1973; Day and Halbach, 1979; Halbach and Chatterjee, 1982; Berman et al., 1986), but the aqueous solution model as defined above is nonlinear. It was possible to employ regression by using a “derivative-free” nonlinear regression program (BMDPAR: distributed by BMDP Statistical Software, Inc.). Equation 3 was used to model  $K_{Fe}$ . The ion-exchange reaction (Reaction 4) was fit to

$$RT \ln K_E = -\Delta H^0 + T\Delta S^0 - (P - P^0)\Delta V^0 - \Delta C_p^0 [T - T^0 - T \ln(T/T^0)] \quad (18)$$

using standard reference conditions  $T^0 = 298$  K and  $P^0 = 1$  bar. For the purposes of regression, some noncritical runs (short duration runs, half-brackets with no opposing half-brackets nearby) were excluded. The resulting fit parameters for  $K_{Fe}$  are  $a = -2.35$ ,  $b = 1000$ , and  $c = 3.55$ . The behavior of the resulting aqueous solution model as a function of  $m_T$  is illustrated in Figure 1. The details of the olivine solution model employed for the purposes of this regression are discussed in a separate section below. However, since the experiments that constrain the value of  $K_{Fe}$  cover such a narrow range of  $X_{fo}$ , the regressed value of  $K_{Fe}$  is not sensitive to the olivine solution model.

Having established values of all parameters of the aqueous solution model, the distribution of electrolyte species was calculated for every experimental run. This allowed calculation of distribution coefficients for the dominant species reaction (Eq. 5). The advantage of this step is that the resulting values of  $K_D^*$  (listed in Table 1 and illustrated in Fig. 4) can be described with a linear thermodynamic model. Linear programming (LP) can then be employed to establish thermodynamic parameters internally consistent with the entire data set.

At equilibrium for Reaction 4, we can write

$$RT \ln K_{D, \text{equil}}^* = -\Delta H^0 + T\Delta S^0 - (P - 1)\Delta V^0 - \Delta C_p^0 [T - T^0 - T \ln(T/T^0)] - RT \ln (\gamma_{fa}/\gamma_{fo}). \quad (19)$$

Each experiment provides a bound on the equilibrium such that either  $RT \ln K_{D, \text{exper}}^* < RT \ln K_{D, \text{equil}}^*$  or  $RT \ln K_{D, \text{exper}}^* > RT \ln K_{D, \text{equil}}^*$ . By substituting experimental conditions and compositions into Equation 19 and noting the direction of approach toward equilibrium, each experiment becomes an inequality constraint on the thermodynamic parameters. However, the absolute bound established by each experiment is not the datum itself,

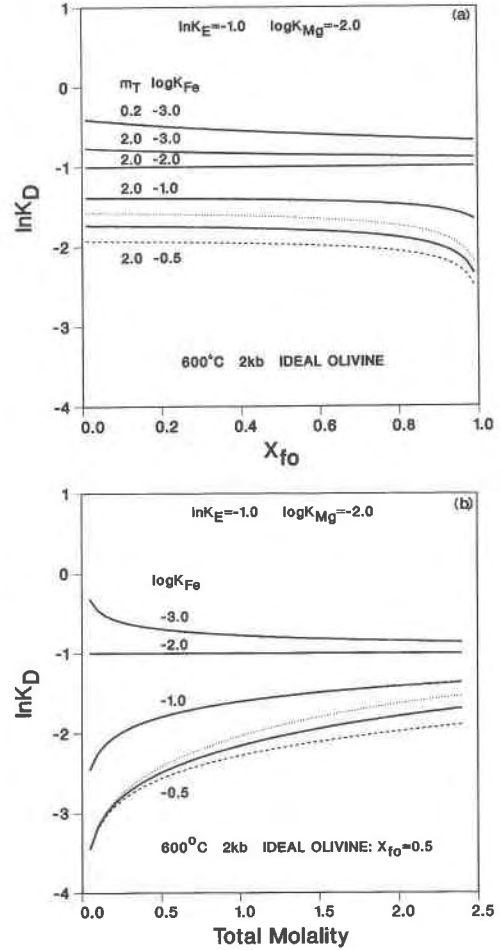


Fig. 3. The effect of variations in  $\log K_{Fe}$  on  $\ln K_D$  as predicted by the aqueous solution model (see text) for the hypothetical case in which the olivine solid solution is ideal. (a)  $\ln K_D$  vs.  $X_{fo}$  at 600 °C, 2 kbar. (b)  $\ln K_D$  vs.  $m_T$  at 600 °C, 2 kbar.

but the corner of its error box that is farthest from the inferred position of the equilibrium. In this study, both final  $X_{fo}$  and  $K_D^*$  were backed off  $2\sigma$  away from the equilibrium prior to calculating the inequality constraints, whereas  $P$  and  $T$  were left at their measured values. The LP calculations were performed with the program LINDO (Linus Schrage, University of Chicago). The thermodynamic expression and the constraints that were employed in modeling the  $\ln \gamma_{fa}/\gamma_{fo}$  term are as follows.

#### The solid solution

A single-site stoichiometric solid solution model was deemed appropriate for the Mg-Fe olivine solid solution since long-range ordering of Mg and Fe in olivine has been shown to be minor or absent (Brown, 1980; Aikawa et al., 1985; de Capitani, 1987). A “Margules” type of formulation was chosen for the sake of comparison. It has been widely applied to silicate solutions following its introduction to the geologic literature by Thompson (1967;

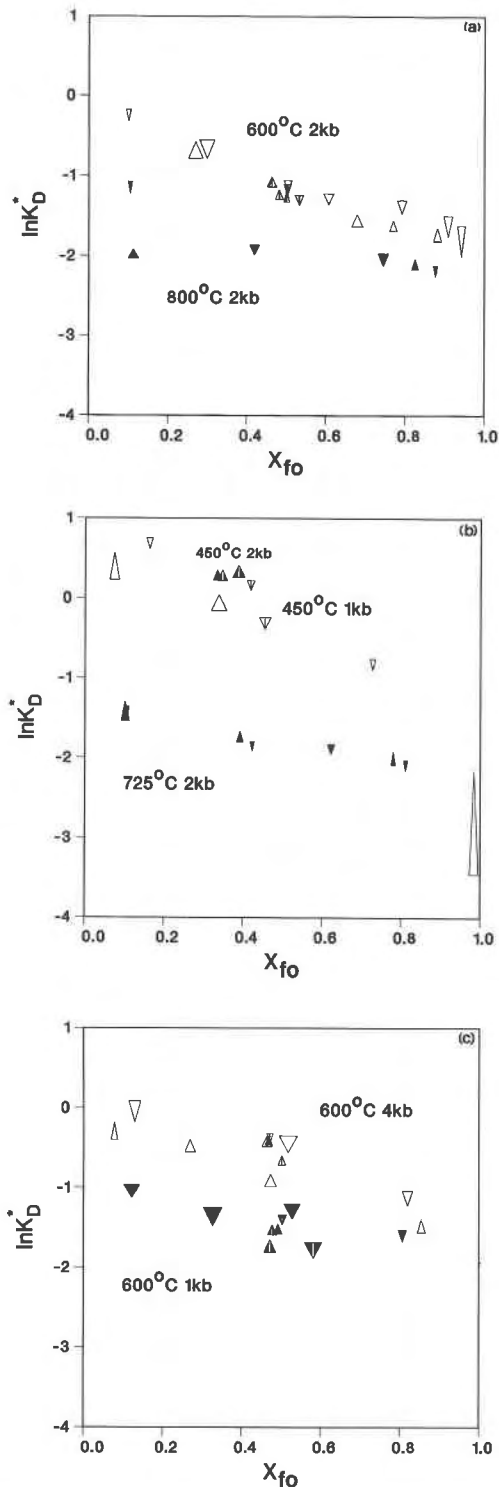


Fig. 4.  $\ln K_D^*$  vs.  $X_{fo}$ : All ion-exchange data recalculated to include only the concentration of the neutral chloride species. See Fig. 1 for explanation of symbols. Symbols containing a vertical line represent experiments with  $m_T < 2m$ . (a) Data at 600 °C (2 kbar) and 800 °C (2 kbar). (b) Data at 450 °C (1 and 2 kbar) and 725 °C (2 kbar). (c) Data at 600 °C (1 kbar) and 600 °C (4 kbar).

see also Grover, 1977; Berman and Brown, 1984). It is also the formulation used in most Mg-Fe olivine solid solution studies previously published.

A second-order, "symmetric" Margules formulation was found most appropriate to model the olivine-aqueous chloride exchange-equilibrium data presented here. The results of taking the natural logarithm of both sides of Equation 6 and substituting in Margules expressions for  $\ln \gamma$  are

$$\ln K_D^* = \ln K_E + 1/RT\{(1 - X_{fo})^2 \cdot [W_{Mg} + 2X_{fo}(W_{Fe} - W_{Mg})] - X_{fo}^2[W_{Fe} + 2(1 - X_{fo}) \cdot (W_{Mg} - W_{Fe})]\} \quad (20)$$

for a third-order, "asymmetric" Margules formulation and

$$\ln K_D^* = \ln K_E + W_G(1 - 2X_{fo})/RT \quad (21)$$

for the symmetric model. Equation 21 is linear in  $X_{fo}$  and Equation 20 describes a curved line in  $\ln K_D^*$  vs.  $X_{fo}$  coordinates. A review of the distribution of data points and their standard errors in Figure 4 shows that a function linear in  $X_{fo}$  is the highest-order polynomial in  $X_{fo}$  that the data seem to require. The single interaction parameter,  $W_G$ , was allowed to vary linearly with  $T$  and  $P$  as follows:

$$W_G = W_H - TW_S + (P - 1)W_V \quad (22)$$

referenced once again to 1 bar and 298 K. The term for excess volume of mixing,  $W_V$ , was held constant at the value of 0.011 J/bar implied by the unit-cell volume data of Schwab and Küstner (1977).

There is very little previously published data that constrain the absolute value of  $W_G$  within or outside of the  $P$ - $T$  conditions of this study. Figure 5 compares published values of  $W_G$  with values implied by the chloride ion-exchange data. Most of the values and models are based upon ion-exchange data that ultimately can constrain only the difference between the solution properties of the two phases involved. Absolute values for individual phases are only obtained when the properties of one phase in each ion-exchange pair are independently known or some assumptions (theoretically sound or otherwise) are made about one phase. The above treatment of the chloride aqueous solution fills this role in the present study. The exceptions to this situation include the solution model of Davidson and Mukhopadhyay (1984) (its  $W_G$  equivalent on Fig. 5), which was obtained from only olivine-olivine ion-exchange data and direct calorimetric measurements (Wood and Kleppa, 1981; Thierry et al., 1981).

Constraints imposed on the Fe-Mg olivine solid solution by calorimetric studies (Wood and Kleppa, 1981; Thierry et al., 1981) were explicitly included as inequality constraints on the value of  $W_H$ . The lead borate solution calorimetry study of Wood and Kleppa (1981) at 970 K was interpreted by the authors to warrant a two-param-



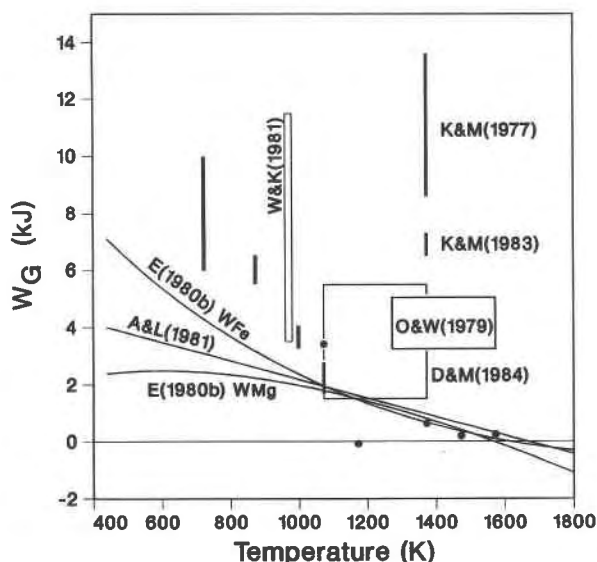


Fig. 5. A compilation of the most recent and most comprehensive measurements of  $W_G$  and Margules solution models for Mg-Fe olivines. The solid dots represent values (no error estimates) from olivine-orthopyroxene ion-exchange experiments as compiled and reinterpreted by Obata et al. (1974). The vertical bars below 1200 K represent  $1\sigma$  error bars about  $W_G$  values produced in the present study by regression of isothermal-isobaric subsets of the data. The remaining authors have been abbreviated as follows: E = Engi, A&L = Andersen and Lindsley, K&M = Kawasaki and Matsui, O&W = O'Neill and Wood, D&M = Davidson and Mukhopadhyay, W&K = Wood and Kleppa (constraints on  $W_H$ ).

eter, "asymmetric" solution model. This cannot be reconciled with the present data set. However, a single-parameter, symmetric model is consistent with the Wood and Kleppa (1981) data at the  $2\sigma$  error level. When the uncertainty in their end-member data is taken into account, their data set constrains  $W_H$  to be between 3.5 and 11.5 kJ at 970 K. The (Na,Li)BO<sub>2</sub> melt calorimetry of Thierry et al. (1981) is consistent with a zero  $W_H$  at 1180 K. However, their uncertainties are so large that  $W_H$  can only be constrained to be between -16 and 16 kJ ( $2\sigma$  errors). This was found to be far from a limiting constraint and was not included.

Figure 6 shows the range of  $W_G$  values allowed by the experimental brackets at each temperature. These are not equivalent to the limits placed upon a model when all of the data are considered together, but still approximately illustrates the region an internally consistent model could occupy. Two solution models were calculated by employing two example objective functions. Because the LP program employed allowed only linear objective functions, a "least-squares" objective function was not possible. Instead, an objective function that minimized the sum of the absolute value of the residuals (with respect to experimental brackets) was used—a "least absolute distance" (LAD) model. The second model, the "minimum" model, was designed to find the most simple thermodynamic

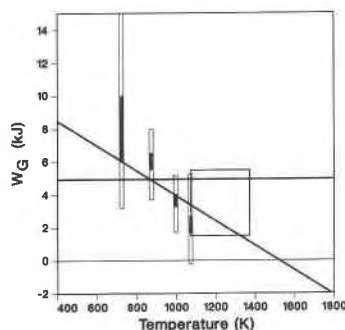


Fig. 6. Comparison of the LAD model and the minimum model with the ion-exchange isotherms and the data of Davidson and Mukhopadhyay (1984). The ion-exchange isotherms are represented both by regression error bars (solid) and absolute limits allowed by  $2\sigma$  bracket expansion (open; calculated by LP).

expression allowed by the data. Its objective function minimized the absolute value of  $W_G$  and  $\Delta C_p^\circ$  of the model exchange reaction (Eq. 4) as well as the sum of the absolute distance residuals. The parameters of the minimum and LAD models are listed in Table 3.

## DISCUSSION

### Fe-Mg olivine

The LAD model is most consistent with all of the pertinent constraints upon the mixing properties of Fe-Mg olivines. However, close scrutiny of the data leads to a number of uncertainties and questions. Figure 6 shows that both models are consistent with the data of Davidson and Mukhopadhyay (1984). However, clearly neither model represents an optimum fit to the chloride ion-exchange data. Even the LAD model shows a systematic misfit characterized by too low a temperature dependence. A review of the model parameters reveals that the LAD model was prevented from acquiring a strong enough temperature dependence (to obtain an optimum fit) by the limit placed upon  $W_H$  by the calorimetric data of Wood and Kleppa (1981). Even if this calorimetric data did not exist and an optimum fit model was allowed there would still be problems. First of all, an optimum fit would be largely inconsistent with the data of Davidson and Mukhopadhyay (1984). In addition, an optimum fit to the chloride data would be characterized by a surprising increase in  $W_G$  with decreasing temperature (leading to unmixing at about 375 °C). In light of all of the problems and inconsistencies of an optimum fit to the chloride data, it is tempting to propose that uncounted factors in the

TABLE 3. Thermodynamic parameters resulting from linear-programming analysis of  $\ln K_0^\circ$  data for Reaction 4

Model	$\Delta H^\circ$ J/mol	$\Delta S^\circ$ J/(K·mol)	$\Delta V$ J/bar	$\Delta C_p^\circ$ J/(K·mol)	$W_H^\circ$ J/mol	$W_S^\circ$ J/(K·mol)
LAD	-90840	-160.9	-2.67	98.2	11500	7.56
Minimum	-66270	-112.2	-2.71	49.9	4940	0.0

behavior of the aqueous solution are responsible for at least part of the fast rise in  $W_G$  implied by the chloride data as treated here.

### The Fe-Mg chloride aqueous solution

An empirical model is established here for the first dissociation equilibrium constant for  $\text{FeCl}_2$  over the pressure and temperature range of the ion-exchange experiments. However, the model fit parameters are poorly constrained by the experimental data and are dependent upon the nature of and assumptions contained in the aqueous solution model as a whole. Most of the data that can constrain the parameters of the aqueous solution model are at 600 °C, but covering a pressure range from 1 to 4 kbar. Therefore, the density coefficient of the  $\text{FeCl}_2$  dissociation model, the  $c$  parameter, is the one most constrained by the experiments. The best fit value, at 3.55, must be identical to the number of water molecules consumed in the dissociation reaction and can be compared within that physical context to the value of 10.6 for  $K_{1,\text{MgCl}_2}$ . The low value for  $K_{1,\text{FeCl}_2}$  could be due to less hydration of  $\text{FeCl}^+$  or greater hydration of neutral  $\text{FeCl}_2$  or both. The two charged species can be expected to have very similar hydration numbers because of the similarity in charge density implied by ionic radii and the presence of only one ligand (identical) in each case. A contrast in hydration of the neutral molecules is more likely because the double ligand allows for the possibility of polar and nonpolar molecular configurations. Accordingly, the contrast in the  $c$  parameter is consistent with a nonpolar  $\text{MgCl}_2$  molecule and a polar configuration for  $\text{FeCl}_2$ .

As suggested above, the surprisingly fast rise in olivine  $W_G$  derived from the ion-exchange data raises questions about the potential of the aqueous solution to contribute to this trend or apparent trend. It has already been demonstrated in Figure 3 that moderate changes in the parameters of the aqueous solution model employed here would have little effect upon the variation of  $K_D$  with composition. Any potential contribution of the aqueous solution to the apparent olivine  $W_G$  must be due to factors omitted from this aqueous solution model or due to inappropriate assumptions and simplifications. If any additional factor is to contribute to the variation in  $K_D$  with composition, it must be something that results in a contrast between the properties of aqueous  $\text{FeCl}_2$  and  $\text{MgCl}_2$ . The aqueous solution model described above includes contrasts in dissociation constants and hydration numbers and provides little support for a contrast in activity coefficients for the charged species. The discussion in the preceding paragraph leads to questions about the assumption of identical (unity) activity coefficients for the neutral chloride species. However, the magnitude of any contrast in activity coefficients could not be independently derived from the present data set.

### Partial molal properties of $\text{MgCl}_2$ and $\text{FeCl}_2$

The difference between the partial molal properties of  $\text{MgCl}_2$  and  $\text{FeCl}_2$  can be calculated by combining the ther-

modynamic model for  $\Delta G_f^0$  with available data on the thermodynamic properties of the end-member olivines. Combining data for forsterite and fayalite from the LP data base of Berman and Greenwood (1985) with the LAD model parameters results in

$$\begin{aligned} \Delta G_f^{\text{MgCl}_2} - \Delta G_f^{\text{FeCl}_2} = & -439\,370 + 189.77T \\ & + 91.76[T - T^0 - T \ln(T/T^0)] \\ & - 2.79(P - P^0) \end{aligned} \quad (23)$$

This equation can be evaluated for consistency with solubility studies involving aqueous  $\text{MgCl}_2$  and  $\text{FeCl}_2$  by taking the difference between model values for  $\Delta G_f^{\text{MgCl}_2} - \Delta G_f^{\text{HCl}}$  from Frantz and Popp (1979) and  $\Delta G_f^{\text{FeCl}_2} - \Delta G_f^{\text{HCl}}$  from Boctor et al. (1980). Figure 7 shows the resulting models at 1 and 2 kbar from the solubility studies along with plots of Equation 23 at 1 and 2 kbar. The slopes of the curves from both data sets are quite similar. The consistent difference of about 15 kJ between the models based upon solubilities and ion-exchange equilibria is worth noting, but is within the combined error estimates for all of the models involved. The most significant contrast is in the dependence of models from the two data types upon pressure. The difference between the 1- and 2-kbar solubility data models is equivalent to a  $\Delta V$  of  $-5.55$  J/mol—twice the value calculated from the ion-exchange data. The true significance of any contrast between models based upon the two data types is difficult to evaluate owing to distinct differences in approaches to modeling distribution of species and activity coefficients in the aqueous solutions.

### Ion-exchange equilibria with aqueous chlorides

In the past, most theoretical interpretations of chloride ion-exchange data have treated the aqueous solution as thermodynamically "ideal" (or its equivalent). Orville (1963, 1972) concluded, on the basis of a few experiments over a range of chloride concentrations (all at 700 °C and 2 kbar), that ion-exchange equilibrium of aqueous chlorides with feldspars was independent of total chloride concentration. Based on this conclusion, he treated the aqueous solution as ideal when interpreting his experiments. Perchuk and Aranovich (1979) based their assumption of ideality in  $\text{AlCl}_3$ - $\text{FeCl}_3$  mixtures on experiments with  $\text{KCl}$ - $\text{NaCl}$  solutions (Perchuk and Andrianova, 1968). Schulien (1980) based his assumption of ideality in  $\text{MgCl}_2$ - $\text{FeCl}_2$  mixtures on a qualitative conclusion that the neutral  $\text{MgCl}_2$  species mixes ideally with  $\text{H}_2\text{O}$  (Frantz and Popp, 1979) and did not attempt to test this assumption experimentally. In contrast, Saxena (1972) analyzed the ion-exchange data of Schulien et al. (1970) by modeling the bulk properties of the  $\text{Mg}$ - $\text{Fe}$  chloride solution with a Margules-type excess function. In doing so he chose to ignore the identity of the actual  $\text{Fe}$  and  $\text{Mg}$  species in the aqueous solution. Thompson and Waldbaum (1968), in analyzing the data of Orville (1963), considered the possibility that  $\text{KCl}$  and  $\text{NaCl}$  are partially dissociated to  $\text{Na}^+$ ,  $\text{K}^+$ , and  $\text{Cl}^-$ . However, they only considered the case in which  $\text{KCl}$  and  $\text{NaCl}$  are dissociated

to the same extent and proceeded to show that this case was indistinguishable from the "ideal solution" assumption when analyzing the ion-exchange equilibrium.

The compilation of supercritical aqueous chloride dissociation data presented in Figure 2 along with observations of the Fe-Mg chloride aqueous solution presented here indicate that more care must be taken in interpreting the results of chloride ion-exchange experiments. The effects of partial dissociation must be taken into account by employing a detailed aqueous solution model. In addition, as discussed above, some uncertainty remains as to whether the aqueous solution model presented here sufficiently accounts for all phenomena that may contribute to "nonideality" in the aqueous solution.

The effects of partial dissociation depend on the value of the dissociation equilibrium constants, and these vary with pressure and temperature. Therefore, the behavior of one chloride compound cannot necessarily be based upon the behavior of another compound, and the behavior of a chloride system at one temperature and pressure cannot be assumed to be identical to its behavior at another temperature or pressure. As illustrated in Figure 3, the contribution of partial dissociation to any apparent variation in  $K_D$  with composition (and the excess free energies of mixing calculated from this variation) is expected to be minor, but not necessarily insignificant. The effective bulk excess free energies of mixing calculated by Pascal and Roux (1985) for KCl-NaCl aqueous solutions at 420 °C and 2 kbar, where both KCl and NaCl are significantly dissociated and significantly dispartate in their dissociation constants, are circa  $-0.5$  kJ at  $X_{\text{Na}} = 0.5$ , which translates to a  $W_G$  (NaCl-KCl) of  $-2$  kJ.

### CONCLUSIONS

A symmetric Margules-type solution model has been developed for Fe-Mg olivines that is based upon new Fe-Mg chloride ion-exchange data from 450 to 800 °C and is consistent with previously published independent constraints. Interpretation of the ion-exchange data included employment of a model for the behavior of the aqueous chloride solution that is as detailed as is warranted by present knowledge of supercritical aqueous electrolytes. Problems with the resulting solid solution model lead to questioning the accuracy of the aqueous solution model. Obtaining accurate solid solution properties from aqueous electrolyte ion-exchange experiments may therefore require putting more effort into characterizing the aqueous solution than the present study. In addition, the accuracy of solid solution properties obtained from previously published chloride ion-exchange experiments must be re-examined in light of the attention paid to the properties of the aqueous solution.

The convenience of aqueous chlorides with respect to interpreting thermodynamic properties of the solid phases from ion-exchange equilibria is questionable at this point in time. It is shown here that a detailed aqueous-electrolyte solution model with an iterative computational solution is required to accurately account for the

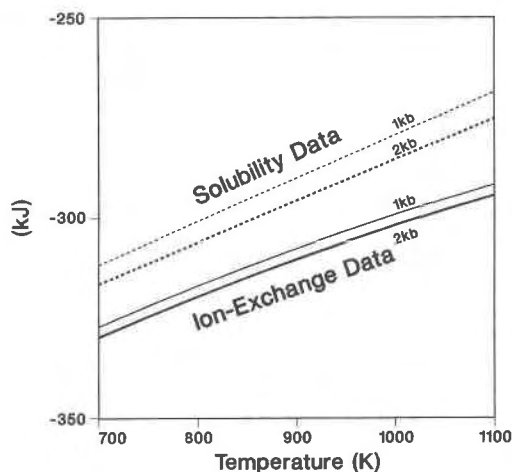


Fig. 7. Comparison of values for  $\Delta G_f(\text{MgCl}_2) - \Delta G_f(\text{FeCl}_2)$  calculated from the present study and from solubility studies.

contribution of the aqueous chlorides to the equilibrium. Assumptions, simplifications, and estimates included in the aqueous solution model owing to lack of empirical data (at the  $P$  and  $T$  of interest here) along with questions raised by the derived solid solution model indicate that the aqueous solution model employed here may be insufficiently detailed and inaccurate.

Despite the computational inconvenience, the potential of aqueous chlorides to be convenient for solid solution studies remains. The empirical data required to construct an accurate aqueous electrolyte solution model can potentially be independently derived through methods such as solution conductivity and solubility studies. The availability of such empirical data is therefore important in choosing solid solutions with potential to be accurately characterized via ion-exchange experiments with aqueous chlorides (or any other aqueous electrolyte).

The experimental convenience of aqueous chlorides is not questioned. Even without the empirical data required to thermodynamically characterize these solutions, they are still useful for studies that compare two solid solutions. This could be either through separate experiments equilibrating the same chloride solution with different solid solutions (characterized by the same exchange couple) or through experiments having both solid phases present plus the aqueous chlorides as a flux.

It is evident that most solid solution properties previously derived from aqueous-chloride ion-exchange studies may be in error. Most of the experimental studies made little or no attempt to test specifically for the contribution of the aqueous solution to the equilibrium. Most theoretical treatments of experimental data treated the aqueous solution as "ideal," or its equivalent. Only the study of Pascal and Roux (1985) is anticipated to be accurate. They employed a detailed aqueous solution model, and an exceptional amount of empirical data is available for the aqueous electrolytes they were using (NaCl, KCl).

## ACKNOWLEDGMENTS

This study is a portion of my dissertation research conducted at the University of British Columbia. Many thanks to Hugh Greenwood for continuous support as well as ideas, advice, and discussions throughout this study. Ideas from and discussions with Martin Engi are greatly appreciated. R. G. Berman, T. H. Brown, E. P. Meagher, and D. McPhail also contributed to fruitful discussions. Bill Persons and Chi-Ming Ip are thanked for help with computer programs. Constructive reviews by B. J. Wood, F. S. Spear, and an anonymous reviewer are greatly appreciated.

## REFERENCES CITED

- Aikawa, N., Kumazawa, M., and Tokonami, M. (1985) Temperature dependence of intersite distribution of Mg and Fe in olivine and the associated change of lattice parameters. *Physics and Chemistry of Minerals*, 12, 1-8.
- Albee, A.L., and Ray, L. (1970) Correction factors for electron probe microanalysis of silicates, oxides, carbonates, phosphates, and sulfates. *Analytical Chemistry*, 42, 1408-1414.
- Andersen, D.J., and Lindsley, D.H. (1979) The olivine-ilmenite thermometer. *Proceedings of the 10th Lunar Planetary Science Conference*, 493-507.
- (1981) The correct Margules formulation for an asymmetric ternary solution: Revision of the olivine-ilmenite thermometer, with applications. *Geochimica et Cosmochimica Acta*, 45, 847-854.
- Bence, A.E., and Albee, A.L. (1968) Empirical correction factors for the electron microanalysis of silicates and oxides. *Journal of Geology*, 76, 382-403.
- Berman, R.G., and Brown, T.H. (1984) A thermodynamic model for multicomponent melts, with application to the system CaO-Al<sub>2</sub>O<sub>3</sub>-SiO<sub>2</sub>. *Geochimica et Cosmochimica Acta*, 48, 661-678.
- Berman, R.G., and Greenwood, H.J. (1985) An internally consistent data base for minerals in the system Na<sub>2</sub>O-K<sub>2</sub>O-CaO-MgO-FeO-Fe<sub>2</sub>O<sub>3</sub>-Al<sub>2</sub>O<sub>3</sub>-SiO<sub>2</sub>-TiO<sub>2</sub>-H<sub>2</sub>O-CO<sub>2</sub>. Atomic Energy Canada Ltd. Technical Report TR-377. Available from SSDO, AECL, Chalk River, Ontario K0J1J0, Canada.
- Berman, R.G., Engi, M., Greenwood, H.J., and Brown, T.H. (1986) Derivation of internally-consistent thermodynamic data by the technique of mathematical programming: A review with application to the system MgO-SiO<sub>2</sub>-H<sub>2</sub>O. *Journal of Petrology*, 27, 1331-1364.
- Boctor, N.Z., Popp, R.K., and Frantz, J.D. (1980) Mineral-solution equilibria: IV. Solubilities and the thermodynamic properties of FeCl<sub>2</sub> in the system Fe<sub>2</sub>O<sub>3</sub>-H<sub>2</sub>-H<sub>2</sub>O-HCl. *Geochimica et Cosmochimica Acta*, 44, 1509-1518.
- Brown, G.E., Jr. (1980) Olivines and silicate spinels. *Mineralogical Society of America Reviews in Mineralogy*, 5, 275-381.
- Chou, I-M., and Eugster, H.P. (1977) Solubility of magnetite in supercritical chloride solutions. *American Journal of Science*, 277, 1296-1314.
- Davidson, P.M., and Mukhopadhyay, D.K. (1984) Ca-Fe-Mg olivines: Phase relations and a solution model. *Contributions to Mineralogy and Petrology*, 86, 256-263.
- Day, H.W., and Halbach, H. (1979) The stability field of anthophyllite: The effect of experimental uncertainty on permissible phase diagram topologies. *American Mineralogist*, 64, 809-823.
- de Capitani, C. (1987) The computation of chemical equilibrium and the distribution of Fe, Mn, and Mg among sites and phases in olivines and garnets. Ph.D. thesis, 259 p. University of British Columbia, Vancouver, British Columbia, Canada.
- Ellis, D.E. (1978) Stability and phase equilibria of chloride and carbonate bearing scapolites at 750 °C and 4000 bar. *Geochimica et Cosmochimica Acta*, 42, 1271-1281.
- Engi, M. (1978) Mg-Fe exchange equilibria among Al-Cr spinel, olivine, orthopyroxene, and cordierite. Ph.D. thesis, 95 p. Swiss Federal Institute of Technology, Zurich, Switzerland.
- (1980a) The solid solution behavior of olivine in the temperature range from 500 K to 1500 K. *Geological Society of America Abstracts with Programs*, 12, 421.
- (1980b) Theoretical analysis of exchange equilibria between a solid solution and an electrolyte fluid undergoing partial association. *Geological Society of America Abstracts with Programs*, 12, 422.
- (1983) Equilibria involving Al-Cr spinel: Mg-Fe exchange with olivine. Experiments, thermodynamic analysis, and consequences for geothermometry. *American Journal of Science*, 283-A, 29-71.
- Franck, E.U. (1956) Hochverdichteter Wasserdampf II. Ionendissoziation von KCl in H<sub>2</sub>O bis 750 °C. *Zeitschrift für Physikalische Chemie, Neue Folge*, 8, 107-126.
- Frantz, J.D., and Marshall, W.L. (1982) Electrical conductances and ionization constants of calcium chloride and magnesium chloride in aqueous solutions at temperatures to 600°C and pressures to 4000 bars. *American Journal of Science*, 282, 1666-1693.
- (1984) Electrical conductances and ionization constants of salts, acids and bases in supercritical aqueous fluids: I. Hydrochloric acid from 100 ° to 700 °C and at pressures to 4000 bars. *American Journal of Science*, 284, 651-667.
- Frantz, J.D., and Popp, R.K. (1979) Mineral-solution equilibria I. An experimental study of complexing and thermodynamic properties of aqueous MgCl in the system MgO-SiO<sub>2</sub>-H<sub>2</sub>O-HCl. *Geochimica et Cosmochimica Acta*, 272, 1223-1239.
- Gordon, T.M. (1973) Determination of internally consistent thermodynamic data from phase equilibrium experiments. *Journal of Geology*, 81, 199-203.
- Grover, J. (1977) Chemical mixing in multicomponent solutions: An introduction to the use of Margules and other thermodynamic excess functions to represent non-ideal behavior. In D.G. Fraser, Ed., *Thermodynamics in geology*, p. 67-97. Reidel, Dordrecht, Netherlands.
- Halbach, H., and Chatterjee, N.D. (1982) The use of linear parametric programming for determining internally consistent thermodynamic data for minerals. In W. Schreyer, Ed., *High-pressure researches in geoscience*, p. 475-491. E. Schweizerbartsche Verlagsbuchhandlung, Stuttgart, West Germany.
- Helgeson, H.C., and Kirkham, D.H. (1974) Theoretical prediction of the thermodynamic behavior of aqueous electrolytes at high pressures and temperatures. II. Debye-Hückel parameters for activity coefficients and relative partial molal properties. *American Journal of Science*, 274, 1199-1261.
- (1976) Theoretical prediction of the thermodynamic behavior of aqueous electrolytes at high pressures and temperatures. III. Equation of state for aqueous species at infinite dilution. *American Journal of Science*, 276, 97-240.
- Helgeson, H.C., Kirkham, D.H., and Flowers, G.C. (1981) Theoretical prediction of the thermodynamic behavior of aqueous electrolytes at high pressures and temperatures: IV. Calculation of activity coefficients, osmotic coefficients, and apparent molal and standard and relative partial molal properties to 600°C and 5 kb. *American Journal of Science*, 281, 1249-1516.
- Kawasaki, T., and Matsui, Y. (1977) Partitioning of Fe<sup>2+</sup> and Mg<sup>2+</sup> between olivine and garnet. *Earth and Planetary Science Letters*, 37, 159-166.
- (1983) Thermodynamic analysis of equilibria involving olivine, orthopyroxene and garnet. *Geochimica et Cosmochimica Acta*, 47, 1661-1679.
- Kitayama, K., and Katsura, T. (1968) Activity measurements in orthosilicate and metasilicate solid solutions. I. Mg<sub>2</sub>SiO<sub>4</sub>-Fe<sub>2</sub>SiO<sub>4</sub> and MgSiO<sub>3</sub>-FeSiO<sub>3</sub> at 1204°C. *Bulletin of the Chemical Society of Japan*, 41, 1146-1151.
- Lagache, M., and Weisbrod, A. (1977) The system Two alkali feldspars-KCl-NaCl-H<sub>2</sub>O at moderate to high temperatures and low pressures. *Contributions to Mineralogy and Petrology*, 62, 77-101.
- Mangold, K., and Franck, E.U. (1969) Elektrische Leitfähigkeit wässriger Lösungen bei hohen Temperaturen und Drucken: II. Alkalichloride in Wasser bis 1000°C und 12 kbar. *Berichte der Bunsengesellschaft*, 73, 21-27.
- Matsui, Y., and Nishizawa, O. (1974) Iron (II)-magnesium exchange equilibrium between olivine and calcium-free pyroxene over a temperature range 800°C to 1300°C. *Bulletin de la Société Française de Minéralogie et de Cristallographie*, 97, 122-130.
- Medaris, L.G., Jr. (1969) Partitioning of Fe<sup>2+</sup> and Mg<sup>2+</sup> between coexisting synthetic olivine and orthopyroxene. *American Journal of Science*, 267, 945-968.

- Nafziger, R.H., and Muan, A. (1967) Equilibrium phase compositions and thermodynamic properties of olivines and pyroxenes in the system  $MgO\text{-}FeO\text{-}SiO_2$ . *American Mineralogist*, 52, 1364–1385.
- Obata, M., Banno, S., and Mori, T. (1974) The iron-magnesium partitioning between naturally occurring coexisting olivine and Ca-rich clinopyroxene: An application of the simple mixture model to olivine solid solution. *Bulletin de la Société Française de Minéralogie et de Cristallographie*, 97, 101–107.
- O'Neill, H.St.C., and Wood, B.J. (1979) An experimental study of Fe-Mg partitioning between garnet and olivine and its calibration as a geothermometer. *Contributions to Mineralogy and Petrology*, 70, 59–70.
- Orville, P.M. (1963) Alkali ion exchange between vapor and feldspar phases. *American Journal of Science*, 261, 201–237.
- (1972) Plagioclase cation equilibria with aqueous chloride solution: Results at 700°C and 2000 bars in the presence of quartz. *American Journal of Science*, 272, 234–272.
- Pascal, M.L., and Roux, J. (1985) K-Na exchange equilibria between muscovite-paragonite solid solution and hydrothermal chloride solutions. *Mineralogical Magazine*, 49, 515–521.
- Perchuk, L.L., and Andrianova, Z.S. (1968) Thermodynamics of equilibrium between alkali feldspar ( $K,Na$ )  $AlSi_3O_8$  with an aqueous solution ( $K,Na$ ) Cl at 500–800°C and 2,000–1,000 bars. In I.Ya. Nekrasov, Ed., *Experimental and theoretical studies of mineral equilibria*, p. 37–72. Nauka Press, Moscow (in Russian).
- Perchuk, L.L., and Aranovich, L.Ya. (1979) Thermodynamics of minerals of variable composition: Andradite-grossularite and pistacite-clinozoisite solid solutions. *Physics and Chemistry of Minerals*, 5, 1–14.
- Quist, A.S., and Marshall, W.L. (1965) Estimation of the dielectric constant of water to 800°C. *Journal of Physical Chemistry*, 69, 3165–3167.
- (1967) A representation of isothermal ion-ion-pair-solvent equilibria independent of changes in dielectric constant. *Proceedings of the National Academy of Sciences*, 58, 901–906.
- (1968) Electrical conductances of aqueous sodium chloride solutions from 0 to 800°C and at pressures to 4000 bars. *Journal of Physical Chemistry*, 72, 684–703.
- Ritzert, G., and Franck, E.U. (1968) Elektrische Leitfähigkeit wässriger Lösungen bei hohen Temperaturen und Drucken: I. KCl, BaCl<sub>2</sub>, Ba(OH)<sub>2</sub> und MgSO<sub>4</sub> bis 750°C und 6 kbar. *Berichte der Bunsengesellschaft*, 72, 798–808.
- Sack, R.O. (1980) Some constraints on the thermodynamic mixing properties of Fe-Mg orthopyroxenes and olivines. *Contributions to Mineralogy and Petrology*, 71, 257–269.
- Sahama, Th.G., and Torgeson, D.R. (1949) Some examples of the application of thermochemistry to petrology. *Journal of Geology*, 57, 255–262.
- Saxena, S.K. (1972) Retrieval of thermodynamic data from a study of inter-crystalline and intra-crystalline ion-exchange equilibrium. *American Mineralogist*, 57, 1782–1800.
- Schulien, S. (1980) Mg-Fe partitioning between biotite and a supercritical chloride solution. *Contributions to Mineralogy and Petrology*, 74, 85–93.
- Schulien, S., Friedrichsen, H., and Hellner, E. (1970) Das Mischkristallverhalten des Olivins zwischen 450° und 650°C bei 1 kb Druck. *Neues Jahrbuch für Mineralogie Monatshefte*, 141–147.
- Schwab, R.G., and Küstner, D. (1977) Precise determination of lattice constants to establish X-ray determinative curves for synthetic olivines of the solid solution series forsterite-fayalite. *Neues Jahrbuch für Mineralogie Monatshefte*, 205–215.
- Sourirajan, S., and Kennedy, G.C. (1962) The system  $H_2O\text{-}NaCl$  at elevated temperatures and pressures. *American Journal of Science*, 260, 115–141.
- Thierry, P., Chatillon-Colinet, C., Mathieu, J.C., Regnard, J.R., and Amosse, J. (1981) Thermodynamic properties of the forsterite-fayalite ( $Mg_2SiO_4\text{-}Fe_2SiO_4$ ) solid solution. Determination of heat of formation. *Physics and Chemistry of Minerals*, 7, 43–46.
- Thompson, J.B., Jr. (1967) Thermodynamic properties of simple solutions. In P.H. Abelson, Ed., *Researches in geochemistry II*, p. 340–361. Wiley, New York.
- Thompson, J.B., Jr., and Waldbaum, D.R. (1968) Mixing properties of sanidine crystalline solutions. I. Calculations based on ion exchange data. *American Mineralogist*, 53, 1965–1969.
- Turnock, A.C., Lindsley, D.H., and Grover, J.E. (1973) Synthesis and unit cell parameters of Ca-Mg-Fe pyroxenes. *American Mineralogist*, 58, 50–59.
- Wellman, T.R. (1970) The stability of sodalite in a synthetic syenite plus aqueous chloride fluid system. *Journal of Petrology*, 11, 49–71.
- Williams, R.J. (1971) Reaction constants in the system  $Fe\text{-}MgO\text{-}SiO_2\text{-}O_2$  at 1 atm between 900 and 1300°C: Experimental results. *American Journal of Science*, 270, 334–360.
- (1972) Activity-composition relations in the fayalite-forsterite solid solution between 900°C and 1300°C at low pressures. *Earth and Planetary Science Letters*, 48, 296–300.
- Wilson, G.A. (1986) Cassiterite solubility and metal chloride speciation in supercritical solutions. Ph.D. thesis, Johns Hopkins University, Baltimore, Maryland.
- Wood, B.J., and Kleppa, O.J. (1981) Thermochemistry of forsterite-fayalite olivine solutions. *Geochimica et Cosmochimica Acta*, 45, 529–534.

MANUSCRIPT RECEIVED DECEMBER 18, 1987

MANUSCRIPT ACCEPTED SEPTEMBER 19, 1988